Bioorganic Chemistry 86 (2019) 696–704

Contents lists available at ScienceDirect

Bioorganic Chemistry

journal homepage: www.elsevier.com/locate/bioorg

Design, synthesis and evaluation of *N*-hydroxypropenamides based on adamantane to overcome resistance in NSCLC

Xuefei Bao[a,1], Yuhong Sun[b,c,1], Changshun Bao[a], Jiayu Zhang[b,c], Shenglan Zou[a], Jingyu Yang[b,c], Chunfu Wu[b,c], Lihui Wang[b,c,*], Guoliang Chen[a,*]

[a] Key Laboratory of Structure-Based Drugs Design and Discovery of Ministry of Education, Shenyang Pharmaceutical University, Shenyang, PR China
[b] Department of Pharmacology, Shenyang Pharmaceutical University, Shenyang, PR China
[c] Benxi Institute of Pharmaceutical Research, Shenyang Pharmaceutical University, Shenyang, PR China

ARTICLE INFO

Keywords:
HDAC
Cisplatin resistance
N-hydroxypropenamide
Molecular docking
Lung cancer

ABSTRACT

A series of novel *N*-hydroxypropenamides containing adamantane moiety were identified and most of them exhibited HDAC inhibitory activity and could reverse the resistance of cisplatin in NSCLC cell lines. In this process, molecular docking was employed to verify the rationality of designing, subsequently, target compounds were synthesized and conducted to enzyme- and cell-based biological evaluation. Most of synthesized compounds could inhibit HDAC activity with the IC_{50} values lower than 50 nM and result in the increase of Ac-H4 and p21 in A549 cells. Importantly, we assessed the reversal effect of those compounds and found several compounds display an anti-resistant effect in lung cancer cells, especially compound **8f**.

As compared to belinostat and cisplatin, compound **8f** showed improved inhibitory activity against A549/CDDP cell lines with IC_{50} value of 5.76 μM, and far lower resistance index of 1.24. Moreover, the structure–activity relationships of these compounds were summarized and compound **8f** could serve as a research tool for identifying the mechanism of reversing resistance and a template for designing novel compounds to reverse cisplatin resistance.

1. Introduction

Non-small cell lung cancer (NSCLC) is the major histologic subtype of lung cancers which is the main cause of cancer-related death worldwide [1]. Although molecular-targeted drugs made a great progress for the treatment of NSCLC in recent years, only patients with specific genetic abnormality benefits from these drugs [2]. The standard therapeutic approach for advanced NSCLC is still conventional cytotoxic drugs-based chemotherapy [3]. Cisplatin (CDDP) is one of the first-line chemotherapeutic agents [4], however, the continuous exposure to CDDP often results in the development of acquired multidrug resistance (MDR) [5,6]. The resistance to CDDP can be caused by numerous mechanisms, such as changes in cellular uptake, drug efflux, increased detoxification, inhibition of apoptosis and increased DNA repair [7,8].

Recently, several studies have shown that the aberrant epigenetic regulations also play a crucial role in cisplatin resistance of NSCLC [9]. In our previous study, we demonstrated that HDAC activity was increased in cisplatin resistant NSCLC cells, suggesting targeting HDAC might be a novel approach to reverse cisplatin resistance in NSCLC [10]. In fact, the previous literature has verified that the inhibition of HDAC might be a promising way to treat drug resistance. Belinostat, a histone deacetylases (HDACs) inhibitor, was approved for the treatment of refractory peripheral *T*-cell lymphoma [11]. It has been reported to circumvent the resistance in NSCLC through inhibition of both ABCC2 and DNA repair-mediated mechanisms [12]. Meanwhile, in our previous work, SNOH-3 derived from belinostat could effectively reverse paclitaxel resistance in non-small cell lung cancer *via* multiple mechanisms [13].

A widely accepted pharmacophore model for HDAC inhibitors consists of a metal binding head group, a linker domain and a cap group, which is a common group for modification [14]. Although a large number of derivatives of belinostat were obtained, the caps of them were almost all aromatic groups. Therefore, non-planar adamantane moieties were employed to replace the terminal phenyl group of belinostat, and the substituted pattern of phenyl linker is changed

* Corresponding authors at: Key Laboratory of Structure-Based Drugs Design and Discovery of Ministry of Education, Shenyang Pharmaceutical University, Shenyang, PR China (G. Chen); Department of Pharmacology, Shenyang Pharmaceutical University, Shenyang, PR China (L. Wang).
E-mail addresses: lhwang@syphu.edu.cn (L. Wang), spucgl@163.com (G. Chen).
[1] These authors contributed equally to the work.

https://doi.org/10.1016/j.bioorg.2019.02.047
Received 7 September 2018; Received in revised form 19 February 2019; Accepted 21 February 2019
Available online 22 February 2019
0045-2068/

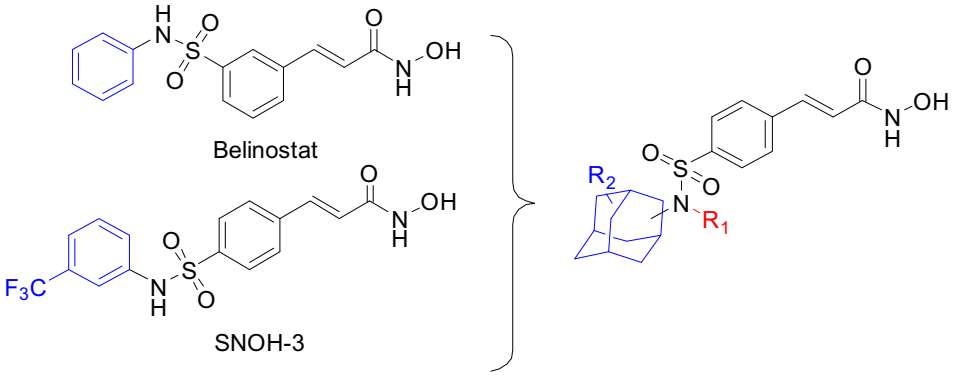

Fig. 1. The design rationale for the final compounds.

from meta-position to para-position (Fig. 1). It was expected to investigate the influence of non-planar cap on inhibitory activity against HDAC, and discovery novel compounds with potential capability to reverse drug resistance in NSCLC. In this paper, we describe the results obtained from the synthesis, docking modeling, enzyme- and cell-based assay on these novel compounds.

2. Results and discussion

2.1. Molecular docking

The docking study revealed that belinostat and **8f** could bind to the same cavity of HDAC1 (PDB ID: 4BKX), with similar binding affinity of −8.28 (XP GScore) and −7.68 (XP GScore), respectively (Fig. 2). The hydroxamic acid group, attached with its aliphatic chain lying in the channel, binds to the zinc atom at the bottom of this channel. There are very similar interactions between the amino acid residues and hydroxamic acid groups of ligands. The ionization of hydroxamic acid groups is favor to form salt bridge, which would stabilize the receptor-ligand complex. However, the hydrogen bonds between belinostat and His178 is missing in terms of **8f**, and the adamantane group of **8f** is close to hydrophobic pocket S, whereas the terminal phenyl of belinostat is solvent exposure. The difference interactions caused by adamantane group may produce different biological activities.

2.2. Chemistry

The route adopted for the preparation of target compounds is depicted in Scheme 1. Cinnamic acid **1**, as the starting material, was reacted with chlorosulfonic acid at 0 °C to furnish (*E*)-3-(4-(chlorosulfonyl)phenyl)acrylic acid **2**, which was subsequently transformed into methyl (*E*)-3-(4-(chlorosulfonyl)phenyl)acrylate **3** *via* reacting with sulfoxide chloride then methanol. Compound **3** was reacted with the corresponding primary amines to afford sulfonamide derivatives **4**, which were transformed into the alkylates **5** *via* reaction with dimethyl sulfate or diethyl sulfate. Next, cinnamic acid derivatives **6** obtained from **4** to **5** were reacted with sulfoxide chloride and then hydroxylamine protected by THP to afford the amide derivatives **7**, and the *N*-hydroxypropenamides **8** were obtained *via* deprotection. The structures of target compounds **8** were characterized by ^{1}H NMR, MS and HRMS.

As for the synthesis of intermediates **4**, the appropriate base was essential. Only a small amount of 4 was obtained *via* column chromatography on silica gel when the reaction was conducted in the presence of triethylamine. The yield of **4** was increased by replacing triethylamine with pyridine. The amount of pyridine also influenced the yield of products. When the amount of pyridine was less than 8 equiv, starting material **3** could be detected by TLC analysis. Considering the large amount of pyridine, we employed it as both solvent and acid binding agent, which could improve the yield and simplify the work-up procedure. The next step was alkylation, which was influenced by solvent. When the substrate was containing terminal phenyl group, satisfactory result was obtained in acetone, while the result of substrate containing

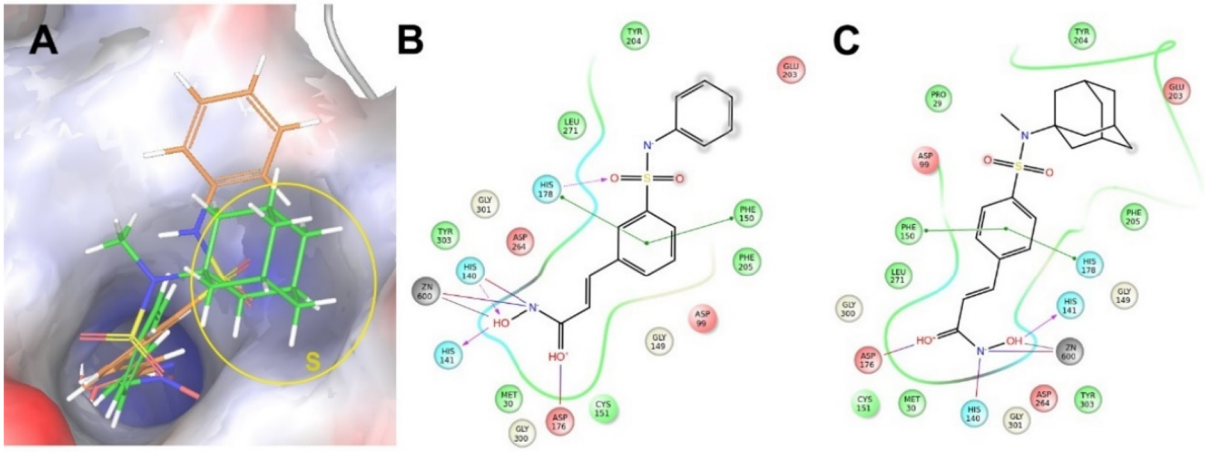

Fig. 2. Molecular docking 3D and 2D models of belinostat and 8f in HDAC1. (A) Docked image of belinostat (orange) and **8f** (green) in the HDAC1 crystal structure (PBD ID: 4BKX). (B) 2D binding model of belinostat with HDAC1. Hydrogen bonds are indicated with purple dashed arrow, pi–pi interaction is indicated with green line, salt bridges is indicated with purple-red line, solvent exposure is indicated with shadow, colour lines around belinostat stand for the binding pocket and the residues in colours nearby established the pocket. (C) 2D binding model of **8f** with HDAC1. (For interpretation of the references to colour in this figure legend, the reader is referred to the web version of this article.)

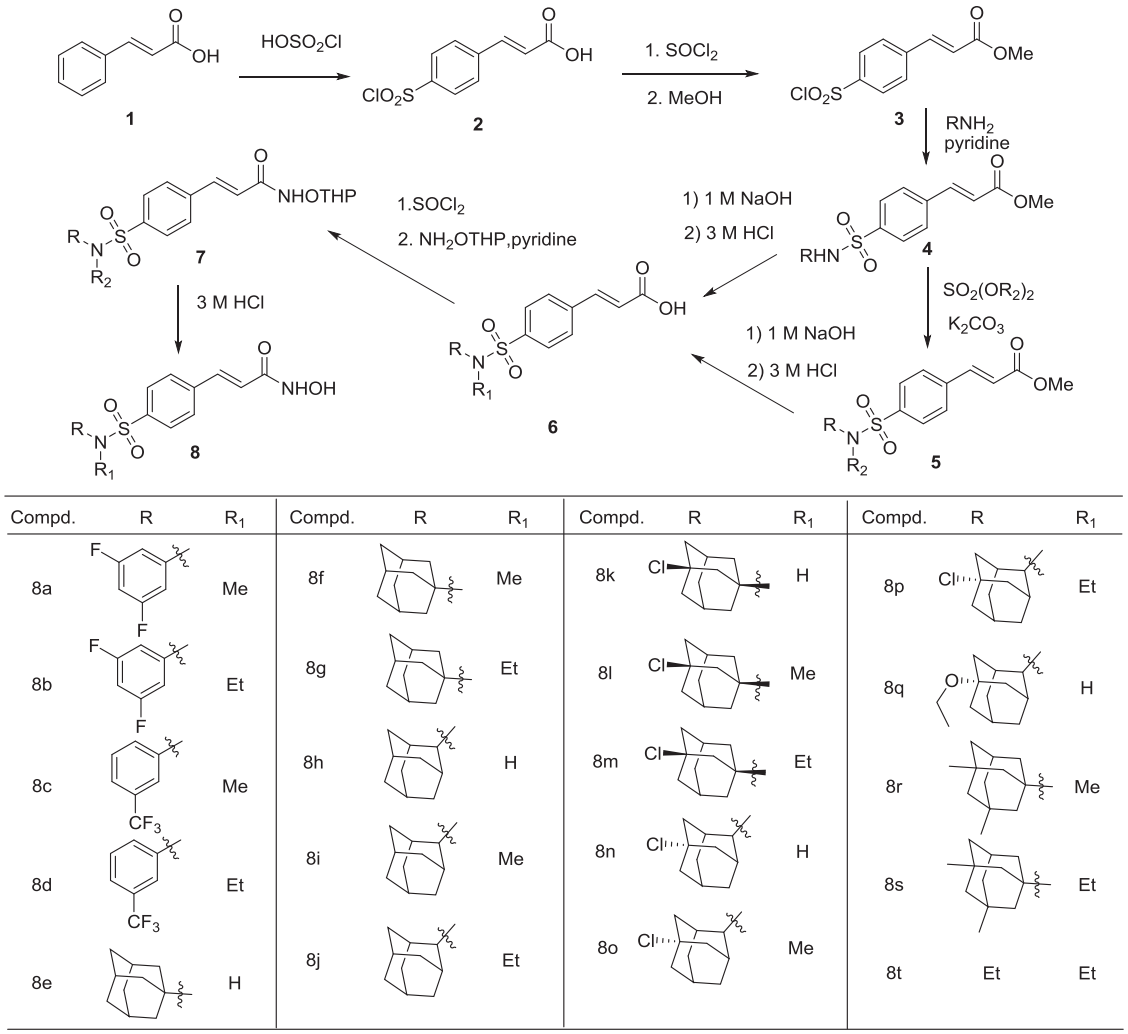

Scheme 1. Synthesis of *N*-hydroxypropenamides incorporating adamantane moiety.

Table 1
The inhibition of synthesized compounds on HDAC activity.

Compounds	IC_{50} ± SEM(nM)	Compounds	IC_{50} ± SEM(nM)
Belinostat	40.1 ± 1.2	8k	29. 2 ± 0.5
8a	49.8 ± 1.5	8l	42.8 ± 0.9
8b	230.1 ± 10.5	8m	43.4 ± 0.6
8c	89.6 ± 6.2	8n	46.8 ± 0.9
8d	315.8 ± 12.5	8o	81.2 ± 2.1
8e	43.7 ± 0.9	8p	35.9 ± 2.4
8f	36.5 ± 1.5	8q	29.2 ± 2.8
8g	33.6 ± 1.2	8r	51.3 ± 4. 6
8h	43.7 ± 4.3	8s	39.6 ± 3.8
8i	189.6 ± 11.6	8t	519.7 ± 22.8
8j	76.5 ± 3.6		

terminal adamantane was poor. We postulated that the poor result might be due to the stereospecific blockade of adamantane. we investigated the influence of the base, other strong bases, such as potassium tert-butoxide and potassium hydroxide, also could not afford satisfactory yields in acetone. Then we replaced acetone with acetonitrile to increase the operating temperature and an improved yield was obtained.

The ^{1}H NMR spectra represented two characteristic signal (1H) that appeared as two broad singlets in the range of 10.89–9.15 ppm corresponding to the (OH) and (NH) of *N*-hydroxypropenamide. Another singlet signal appeared at 7.59–7.88 ppm (1H) corresponding to the (NH) of sulfamide, while the signal disappeared when the (NH) was alkylation. And two doublets (2H) were observed in the range of 7.84–7.55 ppm showing para-disubstituted pattern which is a characteristic of phenyl group. Moreover, the characteristic signal of the alkenyl protons exhibited two doublets at 7.53–7.50 ppm (1H) and 6.59–6.56 ppm (1H) corresponding to trans-alkene. In addition, the signal of adamantane group appeared at 2.20–1.38 ppm.

2.3. HDAC activity study

In order to assess the biological activity of the synthesized compounds, we first measure the HDAC inhibitory action of those compounds. The synthesized compounds could obviously inhibit the HDAC activity with the IC_{50} values lower than 50 nM concentration. Among them, 12 compounds, including **8a**, **8e–h**, **8k–8n**, **8p**, **8q**, **8s** exhibited a similar inhibitory potential with positive compounds Belinostat (Table 1). If the capping group of compounds is phenyl, the introduction of ethyl into the nitrogen would reduce HDAC inhibition activity (**8a** and **8b**, or **8c** and **8d**). But if the capping group is adamantane, small substituents do not influence the HDAC inhibition activity (**8e**, **8f** and **8g**). And Small substitutes on adamantane and substitution sites of adamantane also have no significant effect on the HDAC inhibition activity (Fig. 3).

Furthermore, we evaluated the synthesized compounds on the expression of Ac-H4, which is considered as direct substrate of HDAC, in A549 cells. Western blot data showed that most of these compounds

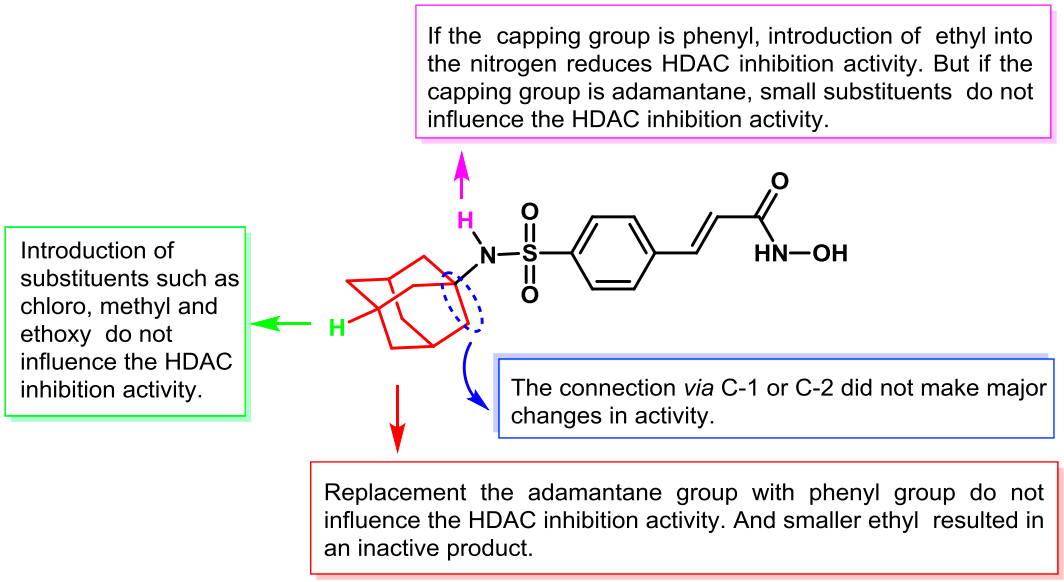

Fig. 3. Structure-activity relationship of compounds according their HDAC inhibition activity.

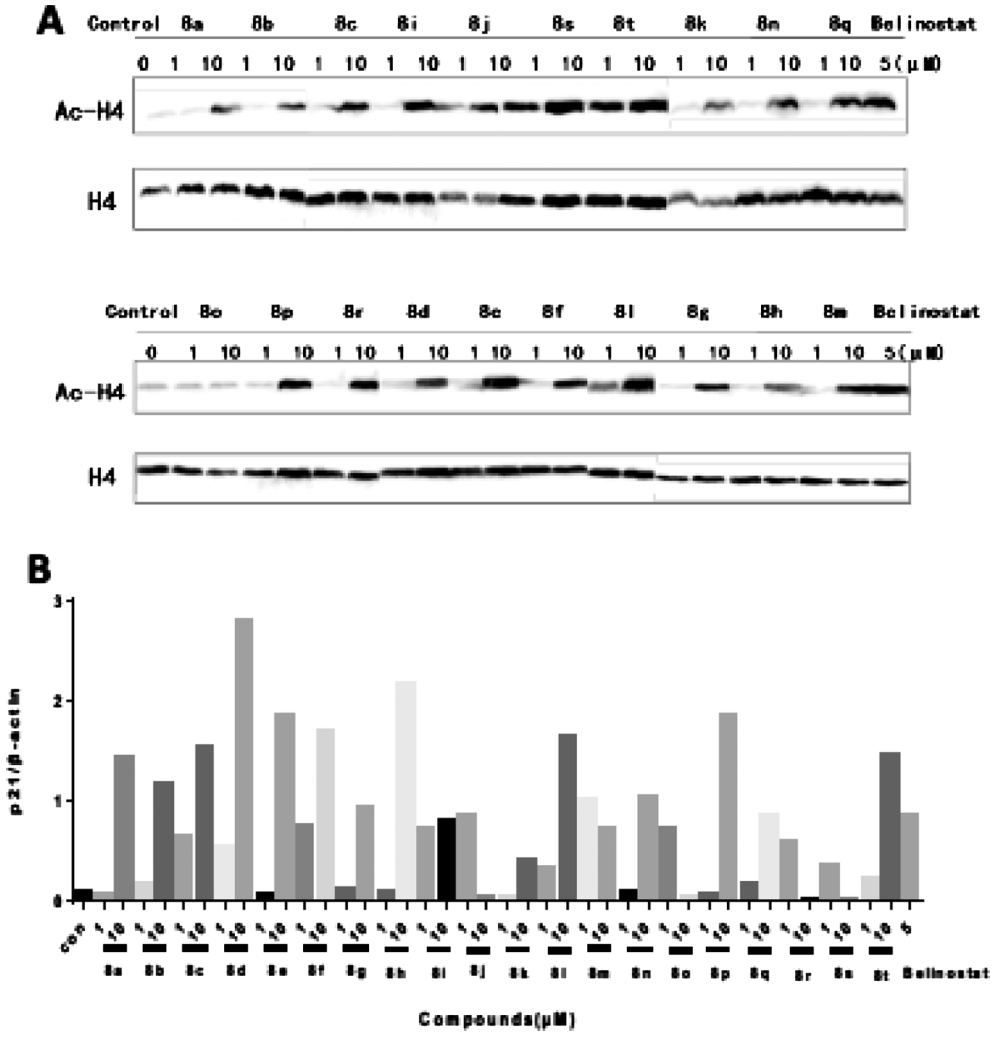

Fig. 4. Expression of Acetylated Histone 4 and target protein p21 in A549 cells after treated with various compounds. **A**. The expression level of Acetylated Histone 4(Ac-H4) was detected by western blot. Histone4 was used as loading control. **B**. The expression level of p21, a HDAC target gene, was detected by western blot and integrated optical density was shown. Actin was used as loading control.

Table 2
Cytotoxicity against several NSCLC cell lines and resistance index of synthesized compounds.

Compd.	Antiproliferative activity IC_{50} ± SEM (μM) and Resistance index for each cisplatin resistance NSCLC cells								
	A549	A549/CDDP	RI*	NCI-H1299	NCI-H1299/CDDP	RI	NCI-H460	NCI-H460/CDDP	RI
8a	0.40 ± 0.03	7.60 ± 1.02	19.00	10.15 ± 2.53	46.64 ± 13.93	4.60	59.58 ± 27.35	71.06 ± 19.26	1.19
8b	2.59 ± 1.03	14.46 ± 2.92	5.58	8.84 ± 2.62	72.52 ± 14.68	8.20	164.18 ± 18.80	77.13 ± 11.23	0.47
8c	1.95 ± 0.43	20.22 ± 5.31	10.37	8.21 ± 3.02	39.64 ± 13.97	4.83	128.38 ± 61.43	135.96 ± 75.15	1.06
8d	3.73 ± 1.01	23.83 ± 2.05	6.39	9.62 ± 1.26	90.58 ± 16.85	9.42	689.50 ± 111.57	241.87 ± 27.15	0.35
8e	3.10 ± 0.15	9.60 ± 2.33	3.10	10.11 ± 1.12	13.62 ± 1.44	1.35	15.62 ± 0.61	209.18 ± 38.68	13.39
8f	4.64 ± 1.15	5.76 ± 0.71	1.24	4.89 ± 0.05	21.64 ± 12.03	4.43	16.00 ± 2.29	17.25 ± 9.96	1.08
8g	5.32 ± 1.51	7.94 ± 1.63	1.49	40.15 ± 9.36	49.01 ± 7.66	1.22	38.74 ± 7.62	110.99 ± 39.85	2.86
8h	0.95 ± 0.27	9.73 ± 1.04	10.24	11.99 ± 3.36	31.33 ± 0.96	2.61	172.43 ± 90.03	27.01 ± 12.83	0.16
8i	22.13 ± 3.91	32.31 ± 3.24	1.46	8.67 ± 1.73	51.90 ± 2.73	5.99	18.34 ± 6.64	42.40 ± 20.13	2.31
8j	9.77 ± 1.80	9.86 ± 1.34	1.01	25.57 ± 1.55	37.37 ± 4.46	1.46	38.08 ± 2.31	103.02 ± 48.21	2.71
8k	1.37 ± 0.71	8.40 ± 3.77	6.13	27.66 ± 5.67	46.21 ± 12.59	1.67	55.06 ± 19.29	62.02 ± 26.01	1.13
8l	7.89 ± 3.77	7.08 ± 1.83	0.90	9.12 ± 2.67	40.00 ± 12.95	4.39	25.32 ± 1.26	21.34 ± 13.08	0.84
8m	4.46 ± 1.40	13.09 ± 3.48	2.93	68.84 ± 26.84	61.06 ± 14.31	0.89	68.35 ± 6.10	50.49 ± 19.63	0.74
8n	2.76 ± 0.81	7.96 ± 0.90	2.88	11.08 ± 4.45	14.61 ± 5.15	1.32	28.78 ± 9.19	18.60 ± 2.50	0.65
8o	6.83 ± 1.56	9.35 ± 2.09	1.37	152.29 ± 13.45	71.53 ± 25.16	0.47	39.24 ± 17.79	75.59 ± 16.19	1.93
8p	7.95 ± 1.25	9.09 ± 2.13	1.14	8.61 ± 0.36	19.34 ± 5.17	2.25	54.98 ± 11.16	46.44 ± 3.69	0.84
8q	2.08 ± 0.58	9.40 ± 2.68	4.52	22.65 ± 3.99	24.11 ± 6.82	1.06	91.59 ± 49.02	123.25 ± 68.07	1.35
8r	13.75 ± 3.45	8.98 ± 1.78	0.65	20.86 ± 7.90	22.62 ± 4.26	1.08	69.243 ± 43.67	19.13 ± 1.24	0.28
8s	6.26 ± 0.59	9.23 ± 2.05	1.47	21.32 ± 2.20	29.14 ± 0.88	1.37	21.53 ± 1.73	36.93 ± 21.45	1.72
8t	12.59 ± 1.40	40.96 ± 4.53	3.25	93.21 ± 15.63	112.15 ± 7.33	1.20	265.98 ± 133.11	97.77 ± 32.77	0.37
Bel	0.24 ± 0.16	8.85 ± 3.47	36.88	135.98 ± 31.63	32.38 ± 18.93	0.24	166.56 ± 31.63	1263.27 ± 61.72	7.58
CDDP	2.33 ± 0.14	16.86 ± 2.21	8.46	18.19 ± 1.70	93.07 ± 2.87	5.11	4.98 ± 0.35	25.81 ± 0.95	5.18

* Resistance Index(RI): the ratio of IC_{50} in resistance cells to IC_{50} in parental cells.

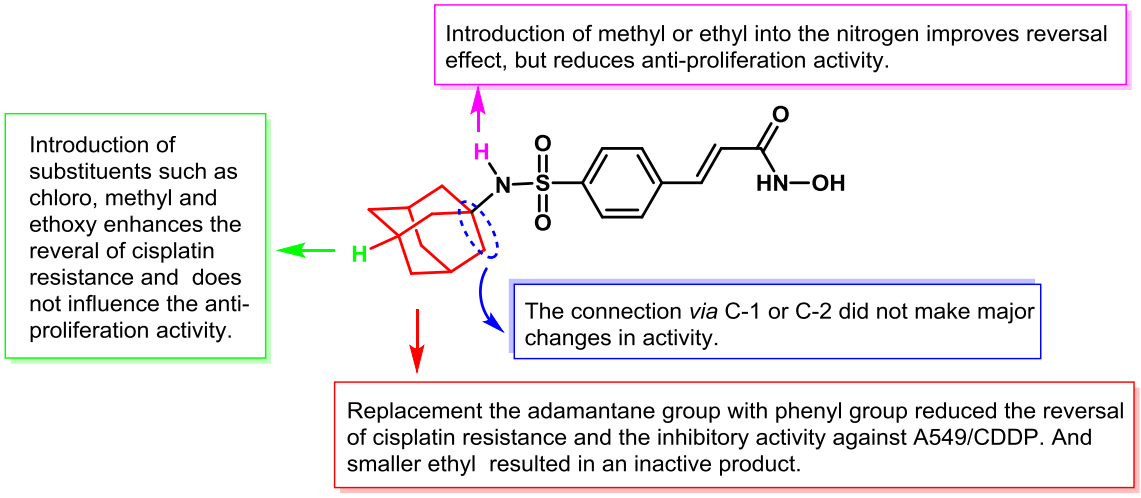

Fig. 5. Structure-activity relationship of compounds according their anti-proliferative effects.

could increase the expression of Ac-H4 at 10 μM concentration, which is consistent with the enzyme-based results (Fig. 4). When the activity of HDAC decrease, chromosome structure will become loose and contribute to gene transcription, such as tumor suppressor gene p21. Thus, we further detected the effect the synthesized compounds on the expression of p21. Our data showed most of these compounds could increase the expression of p21 at 10 μM concentration, which suggested those compounds own the potential of anti-tumor.

2.4. Reversing cisplatin resistance assay

We assessed the synthesized compounds on parental and cisplatin-resistant cells, including A549 and A549/CDDP (A549/cisplatin resistance cells), NCI-H1299 and NCI-H1299/CDDP (NCI-H1299/cisplatin resistance cells), NCI-H460 and NCI-H460/CDDP (NCI-H460/cisplatin resistance cells). For comparison purposes cisplatin and belinostat were used as positive controls. All compounds were treated with NSCLC cells for 48 h and MTT assay was applied to assess the viability of cells. All of IC_{50} values in micromolar (μM) were listed in Table 2. The proliferations of A549, NCI-H460, A549/CDDP and NCI-H460/CDDP were inhibited in a dose dependent manner, and some compounds exhibited the capacity to reverse cisplatin resistance. Moreover, the IC_{50} values of synthesized compounds against A549/CDDP was lower than that of NCI-H460/CDDP. However, these compounds did not show cytotoxicity against NCI-H460 and NCI-H460/CDDP, which was in accordance with the effect of belinostat.

Five of the tested compounds (**8a**, **8f**, **8g**, **8l** and **8n**) showed obvious anti-proliferation effect on A549/CDDP cell lines with IC_{50} values < 8.0 μM, while the IC_{50} values of belinostat and cisplatin were 8.85 μM and 16.86 μM respectively. Specifically, **8f** exhibited eminent growth inhibition against A549/CDDP cell lines with IC_{50} value of 5.76 μM. It was more noteworthy that the resistance index (RI) of **8f** was 1.24, which was far lower than that of belinostat (RI: 36.88) and cisplatin (RI: 8.46). The above results indicated that **8f** was potential to reverse cisplatin resistance in A549 cell lines, and the mechanism of which was distinct from belinostat. Though **8f** showed enhanced anticancer activity against NCI-H1299/CDDP and NCI-H460/CDDP cell lines compared to belinostat and cisplatin, the inhibition strength was

still moderate to low.

Based on the results of anti-proliferation assay against A549/CDDP cell lines, the structure–activity relationship (SAR) could be summarized and demonstrated in Fig. 5. In general, the inhibitory activity against cisplatin resistance cells and the reversal effect were improved when the terminal phenyl groups were replaced by non-planar adamantane groups. While this group was replaced by ethyl (**8t**), a dramatic decrease in activity was observed. And the behavior of small alkyl group on the nitrogen of sulphonamide affected clearly the activity of such derivatives and considered as balancing strategy improving reversal effect but reducing anti-proliferation activity. Compared the inhibitory activity of **8e, 8f** and **8h**, **8i**, the result was shown that the connection position of adamantane influences anticancer activity, and **8f** was the best one. Additional, the introduction of substituents such as chloro (**8n**) and ethoxy (**8q**) at 3-position of the adamantane (**8h**), resulted in a decrease of the RI, which did not influence the anti-proliferation activity. As introduction of more methyl groups (**8r** and **8s**) resulted in a more significant decrease of RI. Therefore, the substituents at the adamantane would benefit the reversal of cisplatin resistance, which might be due to the increase of stereospecific blockade.

3. Conclusions

Firstly, we designed novel compounds based on the knowledge of HDAC, then we verified our design strategy *via* docking these compounds intoHDAC1. Fortunately, molecular docking confirmed the rationality of designing, and these compounds were synthesized. Subsequently, we assessed the effect of the synthesized compounds on HDAC activity in enzyme- and cell-based assay. Finally, because of the complexity of cisplatin resistance, phenotypic screening was employed to evaluate the reversal effect and anti-proliferation activity against cisplatin resistance NSCLC cell lines.

In conclusion, we obtained a series of *N*-hydroxypropenamide derivatives incorporating adamantane moiety with strong reversal effect and potent inhibitory activity against cisplatin resistance A549 cell lines (NSCLC). Compound **8f**, identified by cell-based screening, exhibited obvious reversal of cisplatin resistance with RI of 1.24 and stronger anti-proliferation activity with IC_{50} value of 5.76 μM compared to reference drugs including belinostat and cisplatin. The structure–activity relationship of these compounds was summarized and compound **8f** could serve as a template for designing novel compounds to develop drugs for cisplatin resistance NSCLC.

4. Experimental

4.1. Molecular docking study

All designed compounds were screened by molecular docking using the Glide program (version 10.2, Schrodinger, LLC, New York, 2015). The crystal structure of human HDAC1 (ID: 4BKX) were obtained from the Protein Data Bank (www.pdb.org) and the Protein Preparation Wizard module was applied for the protein structure preparation. The ligands were minimized by means of the LigPrep module. The Glide module was used to generate a receptor grid file that determine the position and size of the active site according the literatures [15], which reported the key amino acids forming the binding pocket. Glide docking was performed using the SP mode with default protocols, and the ligands were treated as flexible. All the docked complexes were scored by the Glide scoring function, and the complexes with higher Glide-score were selected for further analysis of binding mode and critical interactions with the key amino acids.

4.2. Chemistry

All of the starting materials, reagents and solvents are commercially available and used without further purification. Melting points were determined with a X-4 apparatus and were uncorrected. The nuclear magnetic resonance (NMR) spectra were recorded on a Bruker Ascend 400 (Billerica, MA, USA) using tetramethylsilane (TMS) as an internal standard. Electrospray ionization mass spectrometry (ESI-MS) analyses was recorded in an Agilent 1100 Series MSD Trap SL (Santa Clara, CA, USA). The reactions were monitored by thin-layer chromatography (TLC; HG/T2354-92, GF254).

4.2.1. Methyl (E)-3-(4-(chlorosulfonyl)phenyl)acrylate (3)

Compound 3 were prepared according to the literature procedure [16,17].

4.2.2. General procedure for the synthesis of methyl (E)-3-(4-(N-substituted sulfamoyl)phenyl) acrylate derivatives (4)

To a stirred solution of primary amine (7.69 mmol) in anhydrous pyridine (5.0 mL, 61.5 mmol) was added methyl (*E*)-3-(4-(chlorosulfonyl)phenyl)acrylate (2.0 g, 7.69 mmol) solution in anhydrous pyridine (5.0 mL, 61.5 mmol) at 0 °C. The mixture was stirred at 0 °C for 4 h until completion monitored by TLC. The reaction mixture was poured into vigorously stirred 1 N hydrochloric acid (50 mL) and stirred for 1 h. Then the mixture was filtered and washed with water. The residue was dried to produce white solids in 88–99% yields.

4.2.3. General procedure for the synthesis of methyl (E)-3-(4-(N,N-disubstituted sulfamoyl) phenyl) acrylate derivatives (5)

To a solution of 4 (5 mmol) in 10 mL acetonitrile, potassium carbonate (4.1 g, 30 mmol) and dimethyl sulfate/diethyl sulfate (15 mmol) were added and heated under reflux for 17 h. Then the solvent was evaporated under reduced pressure and saturated sodium bicarbonate was added. After string for 30 min, the title compound precipitated and collected by filtering.

4.2.4. General procedure for the synthesis of acrylic acid derivatives (6)

To a solution of 4 or 5 (4.53 mmol) in methanol (20 mL) was added 1 M NaOH (15 mL) and the reaction mixture was refluxed for 2 h. After the completion of the reaction monitored by TLC, the mixture was adjusted to pH 1.0 with 3 N HCl, filtered the precipitated solid, washed with chilled water, and dried to obtain the white crude products 6 in 87–98% yields, which were used in the next step without further purification.

4.2.5. General procedure for the synthesis of isohydroximic acid derivatives (8)

To a solution of cinnamic acid derivative 6 (1.17 mmol) in dichloromethane (10 mL) was added sulfoxide chloride (1 mL, 9.37 mmol) and the reaction mixture was refluxed for 30 min, then the solvent was evaporated under vacuum to get the product cinnamoyl chloride in the form of solid residue in quantitative yield.

Hydroxylamine protected by THP (0.5 g, 4.68 mmol) and anhydrous pyridine (0.5 mL, 5.85 mmol) were dissolved in anhydrous ethyl acetate (10 mL) and stirred at 0 °C. Cinnamoyl chloride was dissolved in dry ethyl acetate (20 mL) and added dropwise to above stirred solution at 0 °C. The reaction mixture was stirred for 10 min, then the reaction mixture was poured into vigorously stirred ice water (100 mL) and extracted with ethyl acetate. The organic layer was washed with brine, dried over magnesium sulfate. Most of the ethyl acetate was evaporated in vacuo, protected hydroxamate was precipitated and collected by filtering.

To a solution of protected hydroxamate (0.38 mmol) in 40 mL of methanol was added 3 N HCl (5 mL) at room temperature. The reaction was monitored by TLC until its completion after stirring for 2 h at 30 °C. The reaction mixture was poured into water (100 mL), filtered the precipitated solid, which was washed with chilled water and dryed to afford target compounds.

*4.2.5.1. (E)-3-(4-(N-(3,5-difluorophenyl)-N-methylsulfamoyl)phenyl)-N-hydroxyacrylamide (**8a**) Light pink solid*

Yield: 95%. mp: 159–162 °C. ^{1}H NMR (400 M Hz, DMSO-d_6): δ (ppm) 10.90 (s, 1H, OH), 9.17 (s, 1H, NH), 7.78 (d, J = 8.24 Hz, 2H, Ar—H), 7.58 (d, J = 8.24 Hz, 2H, Ar—H), 7.52 (d, J = 15.8 Hz, 1H, CH═CH), 7.21 (t, J = 9.24 Hz, 1H, Ar—H), 6.99 (d, J = 8.52 Hz, 2H, Ar—H), 6.60 (d, J = 15.8 Hz, 1H, CH═CH), 3.17 (s, 3H, NCH_3); ESI-MS (m/z): 369.2 $[M+H]^+$, 366.9 $[M-H]^-$.

*4.2.5.2. (E)-3-(4-(N-(3,5-difluorophenyl)-N-ethylsulfamoyl)phenyl)-N-hydroxyacrylamide (**8b**) Light pink solid*

Yield: 61%. mp: 171–172 °C. ^{1}H NMR (400 M Hz, DMSO-d_6): δ (ppm) 10.89 (brs, 1H, OH), 9.16 (brs, 1H, NH), 7.78 (d, J = 7.92 Hz, 2H, Ar—H), 7.62 (d, J = 8.16 Hz, 2H, Ar—H), 7.53 (d, J = 15.76 Hz, 1H, CH═CH), 7.28 (t, J = 9.16 Hz, 1H, Ar—H), 6.94 (d, J = 6.32 Hz, 2H, Ar—H), 6.60 (d, J = 15.76 Hz, 1H, CH═CH), 3.63 (q, J = 6.88 Hz, 2H, NCH_2), 0.99 (t, J = 6.96 Hz, 3H, NCH_2CH_3); ESI-MS(m/z): 383.4 $[M+H]^+$, 405.4 $[M+Na]^+$, 381.2 $[M-H]^-$.

*4.2.5.3. (E)-3-(4-(N-methyl-N-(3-(trifluoromethyl)phenyl)sulfamoyl) phenyl)-N-hydroxyacrylamide (**8c**) Light pink solid*

Yield: 96%. mp: 162–165 °C. ^{1}H NMR (400 M Hz, DMSO-d_6): δ(ppm) 10.89 (brs, 1H, OH), 9.16 (brs, 1H, NH), 7.76 (d, J = 8.4 Hz, 2H, Ar—H), 7.68 (d, J = 7.52 Hz, 1H, Ar—H), 7.60 (t, J = 7.56 Hz, 1H, Ar—H), 7.52 (d, J = 8.4 Hz, 2H, Ar—H), 7.48 (d, J = 15.24 Hz, 1H, CH═CH), 7.45 (m, 2H, Ar—H), 6.59 (d, J = 15.84 Hz, 1H, CH═CH) 3.20 (s, 3H, NCH_3); ESI-MS(m/z): 401.5 $[M+H]^+$, 423.5 $[M+Na]^+$, 399.3 $[M-H]^-$.

*4.2.5.4. (E)-3-(4-(N-ethyl-N-(3-(trifluoromethyl)phenyl)sulfamoyl) phenyl)-N-hydroxyacrylamide (**8d**) Light pink solid*

Yield: 89%. mp: 125–128 °C. ^{1}H NMR (400 M Hz, DMSO-d_6): δ(ppm) 10.88 (brs, 1H, OH), 9.16 (brs, 1H, NH), 7.76 (d, J = 8.04 Hz, 2H, Ar—H), 7.72 (d, J = 7.48 Hz,1H, Ar—H), 7.60 (t, J = 7.96 Hz, 1H, Ar—H), 7.55 (d, J = 8.04 Hz, 2H, Ar—H), 7.52 (d, J = 15.88 Hz, 1H, CH═CH), 7.40 (m, 2H, Ar—H), 6.60 (d, J = 15.84 Hz, 1H, CH═CH), 3.66 (q, J = 6.84 Hz, 2H, NCH_2), 0.97(t, J = 6.96 Hz, 3H, NCH_2CH_3); ESI-MS(m/z): 453.6 $[M+K]^+$, 412.5 $[M-H]^-$.

*4.2.5.5. (E)-3-(4-(N-((3 s,5s,7s)-adamantan-1-yl)sulfamoyl)phenyl)-N-hydroxyacrylamide (**8e**) Light pink solid*

Yield: 81%. mp: 149–152 °C. ^{1}H NMR (400 M Hz, DMSO-d_6): δ(ppm) 10.19 (brs, 1H, OH), 9.39 (brs, 1H, NH), 7.84 (d, J = 7.92 Hz, 2H, Ar—H), 7.73 (d, J = 8.04 Hz, 2H, Ar—H), 7.59 (s, 1H, SO_2NH), 7.50 (d, J = 15.72 Hz, 1H, CH═CH), 6.57(d, J = 15.8 Hz, 1H, CH═CH), 1.91 (s, 3H, CH), 1.68 (s, 6H, CH_2), 1.49 (q, 6H, CH_2); ESI-MS(m/z): 377.1 $[M+H]^+$, 399.1 $[M+Na]^+$, 375.0 $[M-H]^-$.

*4.2.5.6. (E)-3-(4-(N-((3 s,5s,7s)-adamantan-1-yl)-N-methylsulfamoyl) phenyl)-N-hydroxyacrylamide (**8f**) Light pink solid*

Yield: 61%. mp: 115–118 °C. ^{1}H NMR (400 M Hz, DMSO-d_6): δ(ppm) 10.89 (brs, 1H, OH), 9.15 (brs, 1H, NH), 7.80 (d, J = 8 Hz, 2H, Ar—H), 7.74 (d, J = 8.08 Hz, 2H, Ar—H), 7.51 (d, J = 16 Hz, 1H, CH═CH), 6.57(d, J = 15.8 Hz, 1H, CH═CH), 2.92 (s, 3H, NCH_3), 2.00 (s, 3H, CH), 1.93 (s, 6H, CH_2), 1.54 (s, 6H, CH_2); ESI-MS(m/z): 391.1 $[M+H]^+$, 413.1 $[M+Na]^+$, 389.0 $[M-H]^-$.

*4.2.5.7. (E)-3-(4-(N-((3 s,5s,7s)-adamantan-1-yl)-N-ethylsulfamoyl) phenyl)-N-hydroxyacrylamide (**8 g**) Light pink solid*

Yield: 49%. mp: 177–180 °C. ^{1}H NMR (400 M Hz, DMSO-d_6): δ (ppm) 10.87 (brs, 1H, OH), 9.15 (brs, 1H, NH), 7.81 (d, J = 8.24 Hz, 2H, Ar—H), 7.73 (d, J = 8.28 Hz, 2H, Ar—H), 7.51 (d, J = 15.8 Hz, 1H, CH═CH), 6.57(d, J = 15.84 Hz, 1H, CH═CH), 3.46 (q, J_1 = 13.52 Hz J_2 = 6.64 Hz, 2H, NCH_2), 1.98 (s, 3H, CH), 1.90 (s, 6H, CH_2), 1.52 (s, 6H, CH_2), 1.24 (t, J = 6.72 Hz, 3H, NCH_2CH_3); ESI-MS (m/z): 405.1 $[M+H]^+$, 427.1 $[M+Na]^+$, 403.0 $[M-H]^-$.

*4.2.5.8. (E)-3-(4-(N-((1r,3r,5r,7r)-adamantan-2-yl)sulfamoyl)phenyl)-N-hydroxyacrylamide (**8h**) Light pink solid*

Yield: 40%. mp: 172–175 °C. ^{1}H NMR (400 M Hz, DMSO-d_6): δ(ppm) 10.87 (brs, 1H, OH), 9.15 (brs, 1H, NH), 7.84 (d, J = 8.16 Hz, 2H, Ar—H), 7.75 (t, 内含d, J = 8.32 Hz, 2H, Ar—H, 1H, SO_2NH), 7.50 (d, J = 15.88 Hz, 1H, CH═CH), 6.57 (d, J = 15.84 Hz, 1H, CH═CH), 3.21 (brs, 1H, CH), 1.97 (d, 2H, CH), 1.69 (d, 4H, CH_2), 1.62 (d, 4H, CH_2), 1.56 (d, 2H, CH), 1.38 (d, 2H, CH_2); ESI-MS(m/z): 377.1 $[M+H]^+$, 399.1 $[M+Na]^+$, 375.0 $[M-H]^-$.

*4.2.5.9. (E)-3-(4-(N-((1r,3r,5r,7r)-adamantan-2-yl)-N-methylsulfamoyl) phenyl)-N-hydroxyacrylamide (**8i**) Light pink solid*

Yield: 60%. mp: 184–187 °C. ^{1}H NMR (400 M Hz, DMSO-d_6): δ(ppm) 10.89 (brs, 1H, OH), 9.17 (brs, 1H, NH), 7.80 (d, J = 8.36 Hz, 2H, Ar—H), 7.76 (d, J = 8.4 Hz, 2H, Ar—H), 7.53 (d, J = 15.84 Hz, 1H, CH═CH), 6.60 (d, J = 15.84 Hz, 1H, CH═CH), 3.08 (s, 1H, CH), 2.84 (s, 3H, NCH_3), 2.20 (s, 2H, CH), 1.95 (d, 2H, CH), 1.78 (m, 4H, CH_2), 1.63 (d, 4H, CH_2), 1.51 (d, 2H, CH_2); ESI-MS(m/z): 391.2 $[M+H]^+$, 413.2 $[M+Na]^+$, 389.2 $[M-H]^-$.

*4.2.5.10. (E)-3-(4-(N-((1r,3r,5r,7r)-adamantan-2-yl)-N-ethylsulfamoyl) phenyl)-N-hydroxyacrylamide (**8j**) Light pink solid*

Yield: 40%. mp: 171–174 °C. ^{1}H NMR (400 M Hz, DMSO- d_6): δ(ppm) 10.88 (s, 1H, OH), 9.16 (s, 1H, NH), 7.80 (d, J = 8.36 Hz, 2H, Ar—H), 7.75 (d, J = 8.44 Hz, 2H, Ar—H), 7.51 (d, J = 16.04 Hz, 1H, CH═CH), 6.58 (d, J = 15.84 Hz, 1H, CH═CH), 3.46 (s, 1H, CH), 3.40 (q, J_1 = 13.68 Hz J_2 = 6.76 Hz, 2H, NCH_2), 2.15 (s, 2H, CH), 1.75 (s, 6H, CH_2), 1.69 (d, 2H, CH_2), 1.62 (s, 2H, CH), 1.40 (d, 2H, CH_2), 1.15 (t, J = 6.8 Hz, 3H, NCH_2CH3); ESI-MS(m/z): 403.3 $[M-H]^-$.

*4.2.5.11. (E)-3-(4-(N-((1 s,3s,5R,7S)-3-chloroadamantan-1-yl) sulfamoyl)phenyl)-N-hydroxyacrylamide (**8k**) Light pink solid*

Yield: 77%. mp: 155–158 °C. ^{1}H NMR (400 M Hz, DMSO- d_6): δ(ppm) 10.87 (brs, 1H, OH), 9.14 (brs, 1H, NH), 7.88 (s, 1H, SO_2NH), 7.84 (d, J = 8.36 Hz, 2H, Ar—H), 7.74 (d, J = 8.28 Hz, 2H, Ar—H), 7.51 (d, J = 15.8 Hz, 1H, CH═CH), 6.57 (d, J = 15.8 Hz, 1H, CH═CH), 2.09 (d, 4H, CH_2), 1.93 (d, 2H, CH_2), 1.86 (d, 2H, CH_2), 1.66 (d, 2H, CH_2), 1.59 (d, 2H, CH), 1.46 (d, 1H, CH_2), 1.36 (d, 1H, CH_2); ESI-MS(m/z): 411.1 $[M+H]^+$, 433.1 $[M+Na]^+$, 435.0 $[M+2+Na]^+$, 409.1 $[M-H]^-$, 411.0 $[M+2-H]^-$.

*4.2.5.12. (E)-3-(4-(N-((1 s,3s,5R,7S)-3-chloroadamantan-1-yl)-N-methylsulfamoyl)phenyl)-N-hydroxyacrylamide (**8l**) Light pink solid*

Yield: 95%. mp: 153–156 °C. ^{1}H NMR (400 M Hz, DMSO-d_6): δ(ppm) 10.88 (s, 1H, OH), 9.16 (s, 1H, NH), 7.84 (d, J = 8.24 Hz, 2H, Ar—H), 7.76 (d, J = 8.32 Hz, 2H, Ar—H), 7.52 (d, J = 15.8 Hz, 1H, CH═CH), 6.58 (d, J = 15.8 Hz, 1H, CH═CH), 2.92 (s, 3H, NCH_3), 2.34(s, 2H, CH_2), 2.19 (brs, 2H, CH_2), 1.97 (d, 6H, CH_2), 1.84 (d, 2H, CH), 1.46 (t, 2H, CH_2); ESI-MS(m/z): 423.1 $[M-H]^-$, 425.1 $[M+2-H]^-$.

*4.2.5.13. (E)-3-(4-(N-((1 s,3s,5R,7S)-3-chloroadamantan-1-yl)-N-ethylsulfamoyl)phenyl)-N-hydroxyacrylamide (**8m**) Light pink solid*

Yield: 81%. mp: 152–155 °C. ^{1}H NMR (400 M Hz, DMSO-d_6): δ(ppm) 10.88 (s, 1H, OH), 9.16 (s, 1H, NH), 7.82 (d, J = 8.36 Hz, 2H, Ar—H), 7.75 (d, J = 8.36 Hz, 2H, Ar—H), 7.52 (d, J = 15.84 Hz, 1H, CH═CH), 6.58 (d, J = 15.84 Hz, 1H, CH═CH), 3.47 (q, J_1 = 13.48 Hz, J_2 = 6.6 Hz, 2H, NCH_2), 2.29 (s, 2H, CH_2), 2.16(s, 2H, CH_2), 1.94 (d, 6H, CH_2), 1.79 (d, 2H, CH), 1.44 (q, 2H, CH_2), 1.23 (t, J = 6.72 Hz, 3H, CH_2CH_3); ESI-MS(m/z): 437.0 $[M-H]^-$, 439.0 $[M+2-H]^-$.

*4.2.5.14. (E)-3-(4-(N-((1R,3S,5s,7s)-5-chloroadamantan-2-yl)sulfamoyl) phenyl)-N-hydroxyacrylamide (**8n**) Light pink solid*

Yield: 93%. mp: 212–215 °C ^{1}H NMR (400 M Hz, DMSO-d_6): δ(ppm) 10.88 (s, 1H, OH), 9.15 (s, 1H, NH), 7.85 (d, J = 8.08 Hz, 2H, Ar—H), 7.78 (s, 1H, SO_2NH), 7.61 (d, J = 8.68 Hz, 2H, Ar—H), 7.51 (d, J = 15.8 Hz, 1H, CH═CH), 6.58 (d, J = 15.88 Hz, 1H, CH═CH), 3.27

(s, 1H, NHCH), 2.03 (s, 6H, CH_2), 1.98 (s, 1H, CH_2), 1.90 (d, 2H, CH_2), 1.84 (s, 2H, CH), 1.36 (d, 2H, 1H, CH, 1H, CH_2); ESI-MS(*m/z*): 409.0 $[M-H]^-$, 410.9 $[M+2-H]^-$.

*4.2.5.15. (E)-3-(4-(N-((1R,3S,5s,7s)-5-chloroadamantan-2-yl)-N-methylsulfamoyl)phenyl)-N-hydroxyacrylamide (**8o**) Light pink solid*

Yield: 84%. mp: 191–194 °C. ^{1}H NMR (400 M Hz, DMSO-d_6): δ(ppm) 10.91 (s, 1H, OH), 9.17 (s, 1H, NH), 7.82 (d, *J* = 8.28 Hz, 2H, Ar−H), 7.79 (d, *J* = 8.32 Hz, 2H, Ar−H), 7.55 (d, *J* = 15.76 Hz, 1H, CH═CH), 6.61 (d, *J* = 15.88 Hz, 1H, CH═CH), 3.02 (s, 1H, NCH), 2.78 (s, 3H, NCH_3), 2.46 (s, 2H, CH_2), 2.08 (brs, 7H, CH_2), 1.89 (d, 2H, CH), 1.49 (d, 2H, 1H, CH, 1H, CH_2); ESI-MS(*m/z*): 423.6 $[M-H]^-$, 425.0 $[M+2-H]^-$.

*4.2.5.16. (E)-3-(4-(N-((1R,3S,5s,7s)-5-chloroadamantan-2-yl)-N-ethylsulfamoyl)phenyl)-N-hydroxyacrylamide (**8p**) Light pink solid*

Yield: 59%. mp: 128–131 °C. ^{1}H NMR (400 M Hz, DMSO-d_6): δ(ppm) 10.89 (s, 1H, OH), 9.16 (s, 1H, NH), 7.82 (d, *J* = 8.24 Hz, 2H, Ar−H), 7.77 (d, *J* = 8.4 Hz, 2H, Ar−H), 7.52 (d, *J* = 15.8 Hz, 1H, CH═CH), 6.59 (d, *J* = 15.88 Hz, 1H, CH═CH), 3.46 (s, 1H, NCH), 3.36 (q, 2H, NCH_2), 2.39 (s, 2H, CH_2), 2.13 (q, 4H, CH_2), 2.03 (d, 3H, CH_2), 1.69 (d, 2H, CH), 1.39 (d, 2H, 1H, CH_2, 1H, CH); 1.12(t, *J* = 6.8 Hz, 3H, N CH_2 CH_2 CH_3); ESI-MS(*m/z*): 437.2 $[M-H]^-$, 439.1 $[M+2-H]^-$.

*4.2.5.17. (E)-3-(4-(N-((1R,3S,5s,7s)-5-ethoxyadamantan-2-yl)-N-ethylsulfamoyl)phenyl)-N-hydroxyacrylamide (**8q**) Light pink solid*

Yield: 41%. mp: 112–115 °C. ^{1}H NMR (400 M Hz, DMSO-d_6): δ(ppm) 10.89 (s, 1H, OH), 9.16 (s, 1H, NH), 7.81 (d, *J* = 8.4 Hz, 2H, Ar−H), 7.76 (d, *J* = 8.44 Hz, 2H, Ar−H), 7.52 (d, *J* = 15.8 Hz, 1H, CH═CH), 6.58 (d, *J* = 15.84 Hz, 1H, CH═CH), 3.39 (m, 3H, 含NCH, OCH_2), 3.36 (brs, 2H, NCH_2), 2.35 (s, 1H, CH_2), 2.00 (brs, 1H, CH_2), 1.69 (brs, 5H, CH_2), 1.63 (s, 3H, CH), 1.27 (d, 2H, CH_2) 1.14 (t, *J* = 6.76 Hz, 3H, OCH_2CH_3), 1.02 (t, *J* = 7 Hz, 3H, NCH_2CH_3); ESI-MS(*m/z*): 447.2 $[M-H]^-$.

*4.2.5.18. (E)-3-(4-(N-((1r,3R,5S,7r)-3,5-dimethyladamantan-1-yl)-N-methylsulfamoyl)phenyl)-N-hydroxyacrylamide (**8r**) Light pink solid*

Yield: 60%. mp: 164–167 °C. ^{1}H NMR (400 M Hz, DMSO-d_6): δ(ppm) 10.88 (s, 1H, OH), 9.15 (s, 1H, NH), 7.79 (d, *J* = 8.2 Hz, 2H, Ar−H), 7.74 (d, *J* = 8.24 Hz, 2H, Ar−H), 7.51 (d, *J* = 15.8 Hz, 1H, CH═CH), 6.58 (d, *J* = 15.8 Hz, 1H, CH═CH), 2.89 (s, 3H, NCH_3), 2.05 (s, 1H, CH), 1.77 (s, 2H, CH_2), 1.58 (q, 4H, CH_2), 1.20 (q, 4H, CH_2), 1.04 (s, 2H, CH_2), 0.77 (s, 6H, CH_3); ESI-MS(*m/z*): 417.1 $[M-H]^-$.

*4.2.5.19. (E)-3-(4-(N-((1r,3R,5S,7r)-3,5-dimethyladamantan-1-yl)-N-ethylsulfamoyl)phenyl)-N-hydroxyacrylamide (**8s**) Light pink solid*

Yield: 40%. mp: 161–164 °C. ^{1}H NMR (400 M Hz, DMSO-d_6): δ(ppm) 10.88 (s, 1H, OH), 9.15 (s, 1H, NH), 7.79 (d, *J* = 8.36 Hz, 2H, Ar−H), 7.74 (d, *J* = 8.32 Hz, 2H, Ar−H), 7.51 (d, *J* = 15.8 Hz, 1H, CH═CH), 6.57 (d, *J* = 15.88 Hz, 1H, CH═CH), 3.44 (q, J_1 = 13.44 Hz, J_2 = 6.56 Hz, 2H, NCH_2), 2.03 (s, 1H, CH), 1.73 (s, 2H, CH_2), 1.55 (q, 4H, CH_2), 1.22 (t, *J* = 6.56 Hz, 3H, NCH_2CH_3), 1.17 (m, 4H, CH_2), 1.02 (brs, 2H, CH_2), 0.75 (s, 6H, CH_3); ESI-MS(*m/z*): 433.0 $[M+H]^+$, 455.1 $[M+Na]^+$, 431.1 $[M-H]^-$.

*4.2.5.20. (E)-3-(4-(N,N-diethylsulfamoyl)phenyl)-N-hydroxyacrylamide (**8t**) Light pink solid*

Yield: 19%. mp: 132–135 °C. ^{1}H NMR (400 M Hz, DMSO-d_6): δ(ppm) 10.88 (s, 1H, OH), 9.16 (s, 1H, NH), 7.80 (d, *J* = 8.36 Hz, 2H, Ar−H), 7.76 (d, *J* = 8.44 Hz, 2H, Ar−H), 7.52 (d, *J* = 15.8 Hz, 1H, CH═CH), 6.68 (d, *J* = 15.88 Hz, 1H, CH═CH), 3.16 (q, J_1 = 14.16 Hz, J_2 = 7.04 Hz, 4H, CH_2), 1.03 (t, *J* = 7.08 Hz, 6H, NCH_2CH_3); ESI-MS (*m/z*): 297.1 $[M-H]^-$.

4.3. Enzyme-based activity assay

The in vitro HDAC assay was performed with an HDAC fluorescent activity assay kit (BioVision, San Francisco, CA, USA) as our previous reported. Briefly, A549 nuclear proteins were incubated with various concentrations(1 nM to 10 uM) compounds and belinostat at 37 °C for 30 min in the presence of na HDAC fluorimetric substrate. The HDAC assay developer (which produces a fluorophore in reaction mixture) was added, and the fluorescence was measured using a microplate reader (Molecular Devices, Sunnyvale, CA, USA).

4.4. Western blot analysis

About 1×10^7 A549 cells were gathered after pre-treatment compounds for 48 h. Western blotting was performed as previously described. Briefly, an equal amount of total protein extracts from cultured cells or tissues was fractionated by 10–15% SDS-PAGE and then electrically transferred onto polyvinylidene difluoride (PVDF) membranes. Mouse or rabbit primary antibodies(Ac-Histone 4, p21) and appropriate horseradish peroxidase (HRP)- conjugated secondary antibodies were used to detect the designated proteins. The bound secondary antibodies on the PVDF membrane were reacted with ECL detection reagents (Pierce, Rockford, IL, USA) and exposed to X-ray films. Results were normalized to the internal control Histone4 or β-actin.

4.5. Cell viability assay

Human lung cancer cell lines A549, NCI-H1299 and NCI-H460 were obtained from the American Type Culture Collection (Manassas, VA, USA). These cancer cells were routinely cultured in RPMI-1640 or DMEM supplemented with 10% fetal bovine serum (FBS) and maintained at 37 °C in a humidified incubator with 5% CO_2. Specially, the resistance of these lung cancer cells was maintained by continuously exposing to increasing concentrations of cisplatin and later maintain at 200 ng/ml.

3-(4,5-dimethylthiazol-2-yl)-2,5-diphenyl tetrazolium bromide (MTT) was purchased from Sigma. Synthesized compounds and reference agents were dissolved in DMSO to 100 mM and stored at −20 °C. Before treatment, the stock solution is diluted to different concentrations. The final concentration of DMSO in cultures is 0.1% (v/v) or less.

The in vitro cell viability was determined by MTT assay. The cells (1×10^5 cells/ml) were seeded into 96-well culture plates. After overnight incubation maintained at 37 °C in a humidified incubator with 5% CO_2., the cells were treated with various concentrations of agents for 48 h. Then 10 μl MTT solution (2.5 mg/ml in PBS) was added to each well, and the plates were incubated for an additional 4 h at 37 °C. After centrifugation (2500 r.p.m., 10 min), the medium with MTT was aspirated, followed by the addition of 100 μl DMSO. The optical density of each well was measured at 570 nm with a Biotek Synergy HT Reader (Winooski, VT, USA).

Acknowledgements

This work was financially supported by Liaoning Provincial Natural Science Foundation of China (No. 201602707), Scientific Research Fund of Liaoning Provincial Education Department (No. 2017LFW01), Discipline Construction Program of Shenyang Pharmaceutical University (No. 52134606), and National Natural Science Foundation of China (No. 81572947).

Conflict of interest

The authors declare that there is no conflict of interest.

References

[1] R.L. Siegel, K.D. Miller, A. Jemal, Cancer statistics, 2017, CA Cancer J. Clin. 67 (2017) 7–30, https://doi.org/10.3322/caac.21387.

[2] D.S. Tan, S.S. Yom, M.S. Tsao, H.I. Pass, K. Kelly, N. Peled, R.C. Yung, I.I. Wistuba, Y. Yatabe, M. Unger, P.C. Mack, M.W. Wynes, T. Mitsudomi, W. Weder, D. Yankelevitz, R.S. Herbst, D.R. Gandara, D.P. Carbone, P.A. Bunn Jr., T.S. Mok, F.R. Hirsch, The international association for the study of lung cancer consensus statement on optimizing management of EGFR mutation-positive non-small cell lung cancer: status in 2016, J. Thorac. Oncol. 11 (2016) 946–963, https://doi.org/10.1016/j.jtho.2016.05.008.

[3] K.D. Miller, R.L. Siegel, C.C. Lin, A.B. Mariotto, J.L. Kramer, J.H. Rowland, K.D. Stein, R. Alteri, A. Jemal, Cancer treatment and survivorship statistics, 2016, CA Cancer J. Clin. 66 (2016) 271–289, https://doi.org/10.3322/caac.21349.

[4] D.A. Fennell, Y. Summers, J. Cadranel, T. Benepal, D.C. Christoph, R. Lal, M. Das, F. Maxwell, C. Visseren-Grul, D. Ferry, Cisplatin in the modern era: the backbone of first-line chemotherapy for non-small cell lung cancer, Cancer Treat. Rev. 44 (2016) 42–50, https://doi.org/10.1016/j.ctrv.2016.01.003.

[5] Y.P. Liu, C.J. Yang, M.S. Huang, C.T. Yeh, A.T.H. Wu, Y.C. Lee, T.C. Lai, C.H. Lee, Y.W. Hsiao, J. Lu, C.N. Shen, P.J. Lu, M. Hsiao, Cisplatin selects for multidrug-resistant CD133+ cells in lung adenocarcinoma by activating notch signaling, Cancer Res. 73 (2013) 406–416, https://doi.org/10.1158/0008-5472.CAN-12-1733.

[6] L. Wang, X. Liu, Y. Ren, J. Zhang, J. Chen, W. Zhou, W. Guo, X. Wang, H. Chen, M. Li, X. Yuan, X. Zhang, J. Yang, F. Wu, Cisplatin-enriching cancer stem cells confer multidrug resistance in non-small cell lung cancer *via* enhancing TRIB1/HDAC activity, Cell Death Dis. 8 (2016) e2746, , https://doi.org/10.1038/cddis.2016.409.

[7] A.M. Florea, D. Büsselberg, Cisplatin as an anti-tumor drug: cellular mechanisms of activity, drug resistance and induced side effects, Cancers 3 (2011) 1351–1371, https://doi.org/10.3390/cancers3011351.

[8] X. Song, X. Liu, W. Chi, Y. Liu, L. Wei, X. Wang, J. Yu, Hypoxia-induced resistance to cisplatin and doxorubicin in non-small cell lung cancer is inhibited by silencing of HIF-1α gene, Cancer Chemother. Pharmacol. 58 (2006) 776–784, https://doi.org/10.1007/s00280-006-0224-7.

[9] K.J. O'Byrne, M.P. Barr, S.G. Gray, The role of epigenetics in resistance to Cisplatin chemotherapy in lung cancer, Cancers (Basel) 17 (2011) 1426–1453, https://doi.org/10.3390/cancers3011426.

[10] L. Wang, X. Liu, Y. Ren, J. Zhang, J. Chen, W. Zhou, W. Guo, X. Wang, H. Chen, M. Li, X. Yuan, X. Zhang, J. Yang, C. Wu, Cisplatin-enriching cancer stem cells confer multidrug resistance in non-small cell lung cancer via enhancing TRIB1/HDAC activity, Cell Death Dis. 13 (2017) e2746, , https://doi.org/10.1038/cddis.2016.409.

[11] R.M. Poole, Belinostat: first global approval, Drugs 74 (2014) 1543–1554, https://doi.org/10.1007/s40265-014-0275-8.

[12] Kenneth Kin-Wah To, W.S. Tong, L.W. Fu, Reversal of platinum drug resistance by the histone deacetylase inhibitor belinostat, Lung Cancer 103 (2017) 58–65, https://doi.org/10.1016/j.lungcan.2016.11.019.

[13] L. Wang, H. Li, Y. Ren, S. Zou, W. Fang, X. Jiang, L. Jia, M. Li, X. Liu, X. Yuan, G. Chen, J. Yang, C. Wu, Targeting HDAC with a novel inhibitor effectively reverses paclitaxel resistance in non-small cell lung cancer *via* multiple mechanisms, Cell Death Dis. 7 (2016) e2063, , https://doi.org/10.1038/cddis.2015.328.

[14] R. Cincinelli, V. Zwick, L. Musso, V. Zuco, M. De Cesare, F. Zunino, C. Simoes-Pires, A. Nurisso, G. Giannini, M. Cuendet, S. Dallavalle, Biphenyl-4-yl-acrylohydroxamic acids: Identification of a novel indolyl-substituted HDAC inhibitor with antitumor activity, Eur. J. Med. Chem. 112 (2016) 99–105, https://doi.org/10.1016/j.ejmech.2016.02.001.

[15] C.J. Millard, P.J. Watson, I. Celardo, Y. Gordiyenko, S.M. Cowley, C.V. Robinson, L. Fairall, J.W.R. Schwabe, Class I HDACs share a common mechanism of regulation by inositol phosphates, Mol. Cell. 51 (2013) 57–67, https://doi.org/10.1016/j.molcel.2013.05.020.

[16] A. Finn, R. Hollinshead, N. Khan, N. Law, S. Murthy, R. Romero, C. Watkins, V. Andrianov, R.M. Bokaldere, K. Dikovska, V. Gailite, E. Loza, I. Piskunova, I. Starchenkov, M. Vorona, I. Kalvinsh, Novel Sulfonamide Derivatives as Inhibitors of Histone Deacetylase, Helv. Chem. Acta. 88 (2005) 1630–1657, https://doi.org/10.1002/hlca.200590129.

[17] C. Qian, X. Cai, H. Zhai, Preparation of oxazolylmethylthio thiazoles as CDK inhibitors containing a zinc binding moiety [P], WO 2009036016, 2009.